Design and Characterization of Finger-Controlled Micropump for Lab-on-a-Chip Devices

Whulanza, Yudan
Department of Mechanical Engineering, Faculty of Engineering, Universitas Indonesia

Hakim, A. Taufik
Department of Mechanical Engineering, Faculty of Engineering, Universitas Indonesia

Utomo, S. Muhammad
Research Center for Biomedical Engineering, Universitas Indonesia

Irwansyah, Ridho
Department of Mechanical Engineering, Faculty of Engineering, Universitas Indonesia

他

Design and Characterization of Finger-Controlled Micropump for Lab-on-a-Chip Devices

Yudan Whulanza[1,2,*], Taufik A. Hakim[1], Muhammad S. Utomo[2], Ridho Irwansyah[1], Jerome Charmet[3], Warjito[1]

[1]Department of Mechanical Engineering, Faculty of Engineering, Universitas Indonesia, Indonesia 16424
[2]Research Center for Biomedical Engineering, Universitas Indonesia, Indonesia 16424
[3]Institute of Digital Healthcare, WMG, University of Warwick

*E-mail: yudan@eng.ui.ac.id

A microfluidic device that can be operated by simple finger squeezing, without the aid of any extra power, i.e. electricity or a battery, present advantages for diagnostic applications. It is particularly true for diagnostic kits intended to be used in remote areas with limited access to electricity. In this paper, we describe a simple design and manufacturing of a finger pump that relies on an optimised network of check valves and squeeze pumps. The results show that the pump is capable of flowing liquid specimen with a volume of 6 mL with a finger pump priming force of around 3 N. The finger pump is intended to be used in a diagnostic kit.

Keywords: microfluidic device, finger squeeze, diagnostic kit, extra power, remote area

1. Introduction

Over the last decade, due to their capability to integrate multiple laboratory functions into a single chip, microfluidic systems have attracted considerable interest. Microfluidic systems have been widely used in a variety of fields, including analytical chemistry, molecular biology, environmental monitoring and biomedicine systems[1,2]. For example, microfluidic-based micro total analysis system (μTAS) or lab-on-a-chip (LoC) devices have been used for point-of-care-testing (POCT)[3], drug delivery[4], environmental monitoring[5,6] and homeland security[7].

In microfluidic devices, microvalves and micropumps are critical components for the control of fluidic transportation, especially for multi-step chemical reactions or quantitative analysis[8]. A typical micropump enables the precise, accurate and reliable transfer of fluids (biofluid, from a reservoir through the device). One of the most widely used system is the pneumatic-driven micropump, which drives fluid using compressed air. It has the benefits of large displacement and good controllability. Such devices are typically simple and inexpensive and can therefore be used for disposable microfluidic diagnostic systems applications[9,10]. However, reliable high-pressure sources are rarely available in low resources setting. In addition, since we are aiming to design a device for usage in remote area with low electrification, alternative sustainable solutions need

to be considered[11]. Here, we propose a micropump that does not require electricity[12]. The pumping action is provided by the pressure exerted on a membrane to displace volumes of fluid through a valve using finger pressure[13].

A range of finger actuated pumps have been developed to-date, including for droplets delivery in portable digital microfluidics[14] for drug delivery operation[15,16] as well for the dosage of sensitive reagents[17]. This effective pumping method requires reliable microfabrication technology, such as photolithography, to realise the network of microchannels, microvalves and micropump components[18]. However, this fabrication method requires relatively expensive equipment and may not be available in low-resource settings laboratories.

In previous work, we have demonstrated the use of conventional computer numerical control (CNC) milling to fabricate a polymerase chain reaction module[19] as well as cells-on-chip devices and human lung models[20–22]. CNC milling is widely available and compatible with medium-scale manufacturing. This manuscript describes the design and characterisation of a finger-driven micropump fabricated using CNC milling. It is foreseen that such a pump can be seamlessly integrated with our polymerase chain reaction (PCR) detection chip[23].
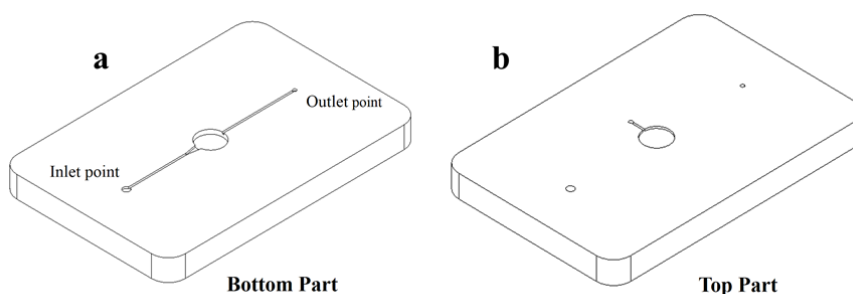
Fig. 1: (a) The micropump's driven fluid channel (bottom part) and the (b) micropump's accumulated driving fluid channel (top part).

2. Methodology

2.1 Design Consideration

Single chamber micropump capable of reaching average flow rates of 20 μL/min have been reported previously[24]. Such devices are comprised of three layers; the pneumatic layer, the thin membrane layer and the liquid layer. With a desired chip size of 10 x 30 mm, the length of the liquid layer channel should be 20 mm to enable fluid flow characterisation. The size of the diaphragm can be altered to accommodate for the size of a finger.

2.2 Design and Simulation

The design of the micropump was supported by a set of calculations and simulation to simulate the pumping mechanism. The two part moulds were designed by a SolidWorks™, a Computer Aided Design (CAD) software. For the simulation, the mutliphysics simulation package COMSOL Multiphysics™ version 5.1 was used.

2.3 Fabrication

The fabrication of the micropump consisted of three steps: mould fabrication, polydimethylsiloxane (PDMS) casting and curing, and product assembling. The aluminium mould was formed using a milling process. Aluminium 7075 was chosen rather than copper due to its economic value, good fatigue strength, ease of machining, good thermal conductivity and low corrosion rate. To achieve a high-precision manufacturing process, an EMCO VMC 200 (Germany) milling machine with a demonstrated accuracy of 1/100 mm was used. We used three types of flat-end mill tools with diameters of 4 mm, 2 mm and 1 mm (Seco Tools, Singapore). The spindle rate was set to 3500 RPM and the feed rate to 50 pps. At the beginning of the process, the milling process was simulated in the CAM programme based on the CAD designs.

For PDMS casting and curing, PDMS (Sylgard 184 silicone; Dow Corning, USA) was casted in the mould. The PDMS was mixed with curing agent at a ratio of 10 to 1. Then, the mould was put under vacuum in a dessicator to remove air trapped in the PDMS during the mixing process. A vacuum pump VE115N (China), was employed for 45 minutes. Afterwards, the mould was put in an oven for 15 minutes at 140°C and then peeled.

For the PDMS membrane, a similar mixture of PDMS was casted onto a spin coater. The spin coater operated for 30 seconds at 2,500 RPM to achieve a membrane with a thickness of around 50 μm. Later, this casted PDMS was placed into an oven for 5 minutes at a temperature of 80°C. For the micropump assembly, the PDMS top and bottom were bonded with the membrane in a series of steps. The bonding process was carried out using a Corona SB plasma treater from BlackHole Lab (France) for 30 seconds for each surface.

2.4 Measurement and Testing

Geometry measurement

In order to evaluate the dimensions of the moulds and PDMS replica, we have used a Dinolite AM 4113 ZT digital microscope (Anmo Electronics, Taiwan). The measurements were taken at 20x magnification to cover the relevant physical dimensions of micropump parts such as the diaphragm and the channel for the top and bottom layers.

Functional testing

The flow displacement and force measurements were characterised by pump priming the micropump module using a micrometer gauge to control the depression of the membrane. The travel distance of the liquid in the channel was then observed and measured. The local fluid displacement was also evaluate using a TerufusionR syringe pump from Terumo, (Japan) operating at a constant flow rate of 5.0 mL/h.

Velocity measurement

The velocity of liquid in the channel was measured using image processing. The position of fluid-air interface (meniscus) in the channel was captured every second. The fluid velocity was calculated by dividing the distance travelled during the observed time. The observation distance, from inlet to outlet, was 20mm.

3. Result and Discussion

3.1 Design of the Micropump

The design in Figure 1 shows the bottom part (left), where the liquid is driven from inlet to outlet and the top part (right) shows the reservoir where the pressurised air is accumulated. The pump should provide enough pressure to the membrane, sandwiched between top and bottom parts, to be deflected and generate fluid flow through the valve. The depths of both top and bottom parts were designed at 2.5 mm whereas the depth of the channel was at 0.2 mm. The width of the channel was designed at 0.2 mm, except in the valve section where the channel enlarges to prevent the backflow of liquid during pumping[5]. The circular reservoir has a diameter of 3 mm and thickness of 0.2 mm. Additionally; the top part also has circular pocket matched with the reservoir in the bottom part with similar dimension of diameter and thickness.
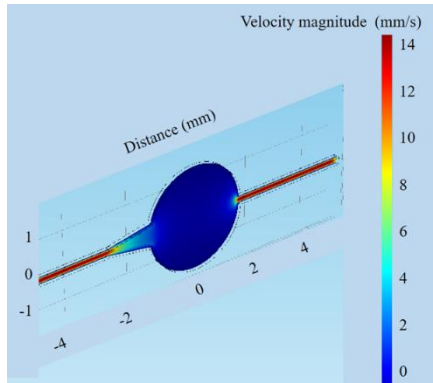
3.2 Numerical Simulation

Fig. 2: Driven fluid channel for the micropump which shows velocity magnitude along the path

Simulations were performed to evaluate the flow in the device. In the simulation environment, a load was delivered onto the sandwiched membrane from top to bottom to emulate the downward movement of a finger. Thus, it delivered pressure to the fluid chamber through a deflection of the membrane. The simulation showed the characteristics of the fluid flow along the microchannel. It provided the liquid velocity magnitude and pressure distribution in the microchannel.

The simulation shows that the velocities were around 12–14 mm/s at the inlet and outlet and 2-6 mm/s in the chamber as shown in Figure 2. A good match between the inlet and outlet velocities is expected in the absence of friction during pumping. The simulation also provided information about the pressure distribution in the device and confirmed that the fluid flows to the outlet as expected (not shown).

3.3 Fabrication Result

In this section we describe the fabrication and assembly of the 3 part PDMS device. As expected, the driving fluid and driven fluid channels were successfully fabricated using a mould transfer method (using the top and bottom part moulds respectively). The thin membrane with uniform thickness was fabricated using a spin coater. The membrane was then sandwiched between the driving fluid channel and the driven fluid channel to form the complete chip product after bonding (Figure 3). The integrity of the device was verified by pumping an aqueous solution. No leaks were detected for flow rates up to 5.0 mL/h.

We have used optical measurement to evaluate the dimensions of the fabricated chip (Figure 3). We used a Dino-Lite™ digital microscope (Taiwan) as in our previous work[22] and noted deviations compared to the design. Table 1 shows the dimensions of the design, mould and chip product. Deviations of 15%, 10% and 4% were noted for the thickness, inlet and outlet width and diaphragm radius respectively. We attribute these deviations to the capability of the CNC machine and the dimension of the tool used. Note that we have used a conventional CNC machine instead of a CNC micromilling machine. Therefore, in the future, a correction factor of around 10-15% needs to be considered during the design.
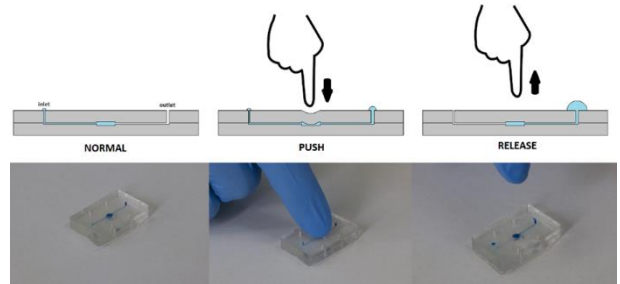
3.4 Flow Testing

Fig. 3: Finger-controlled pumping principle with liquid flow inside the channel

Table 1. Fluid channel geometry (mm)

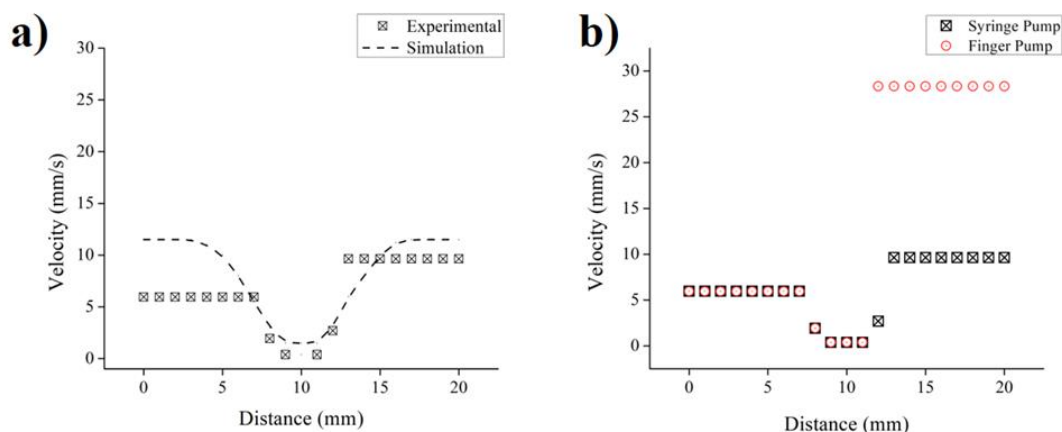|	Channel thickness	Channel width	Diaphragm radius
Design	0.20	0.20	3.00
Mould	0.26 ± 0.05	0.25 ± 0.03	3.28 ± 0.08
Chip product	0.23 ± 0.02	0.23 ± 0.03	2.89 ± 0.04

Fig. 4: a) Velocity profile of liquid in the microchannel in the flow test experiment using external pump; b) Comparing the previous flow test using external pump with finger primping pump

Two scenarios for chip functional testing were employed. First, flow testing in the driving fluid channel was performed using an external syringe pump. This test was carried out to characterise the flow velocities in different parts of the device. The initial flow rate was set at 5.0 mL/h. and the flow velocity was calculated by dividing the distance travelled by the given time interval in between each measurement. The measurements, using a digital microscope, were performed along the entire 20 mm of the channel.

A Terufusion[R] syringe pump from Terumo, Japan provided relatively constant pressure during the testing, therefore enabling us to achieve a velocity profile of driven fluid flow along the channel. Figure 4a shows a constant velocity at the inlet port of around 6 mm/s, which then drops significantly after flowing into the driving fluid reservoir. Later, the velocity increases to around 10 mm/s after the reservoir until the outlet. These velocity figures are consistent with the continuity behaviour of a compressible liquid. The relatively constant velocity indicates that there is no resistance in the channel, which means that the product is well designed. The exit velocity is larger than the inlet velocity due to the design of the opening, which will favour fluid flow towards the outlet.

A dashed line is also plotted in the figure 4a to compare the velocity from experimental with simulation result in previous section. The simulation shows an ideal condition of velocity profile in a microfluidic channel. In the simulation environment, the velocity at the inlet and outlet were at 12 mm/s and decrease down to 1 mm/s in the resrvoir. This decreasing velocity, due to the larger area in the reservoir agrees well with the experimental results (around 1 mm/s).

In second phase of experiment, a finger pumping priming was introduced as shown in Figure 4b. It can be seen that the velocities at the inlet port and reservoir are similar compared to the results obtained with the syringe pump. However, the velocity increases to around 28 mm/s after passing the fluid reservoir. This indicates that the force accumulates until it overcomes the resistance of the channel. based on the observations, we have estimated that the pressure from the finger resulted in a 300% increase in compared to the syringe pumping.

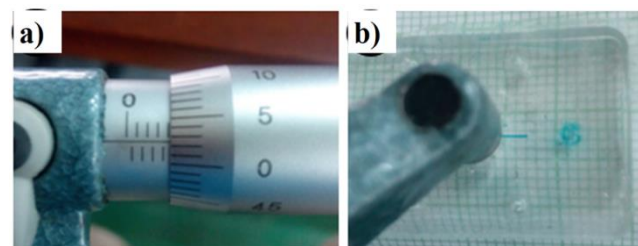### 3.5 Pump Displacement Testing

Fig. 5: a) Micrometer is set in to pinch the chip in the pneumatic pumping area; b) The pinching drives the pneumatic downward to push the liquid in the channel.

In this test, the pump chip were pinched using the micrometer screw gauge, to measure the membrane displacement (figure 5a) and calculate the pumping force. Figure 5b shows the distance travelled by the liquid during the pinching of the membrane using the micrometer screw gauge.

Using the relation between the stiffness of the material (equation 1), the pumping force can be estimated by measuring the axial displacement of the membrane (as indicated by the micrometre gauge). The distance was observed every 1 mm and the volume of fluid (V) calculated using the channel dimensions (estimated to have a uniform area).

The stiffness constant is calculated using equation 1 (below). The area and length of the exposed elements are 7 mm^2 and 4 mm, respectively according to the dimension of pump diaphragm. Taking the Young's modulus of 2.5 MPa for PDMS[25], the stiffness constant was calculated at

4.4 MPa.mm. We then calculated the force by multiplying the stiffness with the displacement of the micrometer gauge (equation 2).

The displacement of pumping fluid was measured in interval of 1 mm (between 0–9 mm in total) The calculated pumping force as a function of the fluid displacement is shown in figure 6a. It can be seen that 3 N is necessary to move the fluid a 9 mm along the channel. Moreover, the minimum force of 1.8 N to get the fluid in motion agrees well with the work of Xiang et al. who also reported a force of about 2 N to squeeze a similar pump[10].
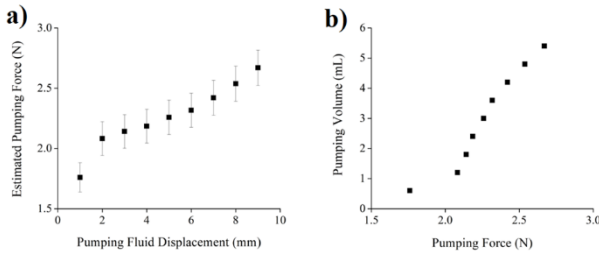

Fig. 6: a) Result of metering fluid displacement with the corresponded estimated force; b) Result of the pumping force with its correlated pumping volume along the channel

Figure 6b replots the previous figure to depict the liquid volume as a function of pumping force. The pumping volume that can be delivered is 1-6 mL with corresponded pumping force between ~1.8 and 3 N. However it is noted that the relation between these two values are not linear. The initial point has a rather high deviation compare to others. It can be attributed to a high flow resistance to overcome the capillary forces.

$$k = \frac{AE}{L} \tag{1}$$

Where:
A is the cross-sectional area of the chip
E is the Young's Modulus of PDMS
L is the length of the exposed element
k is the stiffness constant

$$F = k\delta \tag{2}$$

Where:
F is the force
δ is the screw displacement

4. Conclusion

The manuscript presented the design and characterisation of a finger actuated micropump. The micropump functioned as expected, despite fabrication-induced geometry deviations of up to 15% compared to the design. The micropump testing demonstrated that there was no backflow during the stroke testing and that it was capable of dosing a volume by delivering a 2-3 N force to the membrane. It is foreseen that the micropump can be used in the future development of diagnostic chip system.

References

1) Ni J, Li B, Yang J. A pneumatic PDMS micropump with in-plane check valves for disposable microfluidic systems. *Microelectron Eng.* 2012;99:28-32. doi:10.1016/J.MEE.2012.04.002

2) Charmet J, Arosio P, Knowles TPJ. Microfluidics for Protein Biophysics. *J Mol Biol.* 2018;430(5):565-580. doi:10.1016/J.JMB.2017.12.015

3) Iwai K, Shih KC, Lin X, Brubaker TA, Sochol RD, Lin L. Finger-powered microfluidic systems using multilayer soft lithography and injection molding processes. *Lab Chip.* 2014;14(19):3790. doi:10.1039/C4LC00500G

4) Kleinstreuer C, Li J, Koo J. Microfluidics of nano-drug delivery. *Int J Heat Mass Transf.* 2008;51(23-24):5590-5597. doi:10.1016/J.IJHEATMASSTRANSFER.2008.04.043

5) Marle L, Greenway GM. Microfluidic devices for environmental monitoring. *TrAC Trends Anal Chem.* 2005;24(9):795-802. doi:10.1016/J.TRAC.2005.08.003

6) Lin Y, Timchalk CA, Matson DW, Wu H, Thrall KD. Integrated Microfluidics/Electrochemical Sensor System for Monitoring of Environmental Exposures to Lead and Chlorophenols. *Biomed Microdevices.* 2001;3(4):331-338. doi:10.1023/A:1012417000516

7) Gad-el-Hak M. The Fluid Mechanics of Microdevices—The Freeman Scholar Lecture. *J Fluids Eng.* 1999;121(1):5. doi:10.1115/1.2822013

8) Au AK, Lai H, Utela BR, et al. Microvalves and Micropumps for BioMEMS. *Micromachines.* 2011;2(2):179-220. doi:10.3390/mi2020179

9) Jang L-S, Li Y-J, Lin S-J, et al. A stand-alone

peristaltic micropump based on piezoelectric actuation. *Biomed Microdevices*. 2007;9(2):185-194. doi:10.1007/s10544-006-9020-8

10) Pramanick B, Dey PK, Das S, Bhattacharyya TK. *Design and Development of a PDMS Membrane Based SU-8 Micropump for Drug Delivery System*. Vol 2.; 2013. www.isssonline.in/journal/02paper01.pdf. Accessed March 18, 2019.

11) Sato T. How is a Sustainable Society Established? : A Case Study of Cities in Japan and Germany How is a Sustainable Society Established? A Case Study of Cities in Japan and Germany. *Evergreen*. 2016;3(2):25-35. doi:10.5109/1800869

12) Gima H, Yoshitake T. A Comparative Study of Energy Security in Okinawa Prefecture and the State of Hawaii. *Evergreen*. 2016;3(2):36-44. http://www.tj.kyushu-u.ac.jp/leading/en/c_publication/EG2016-3-2content/Pages 36-44.pdf. Accessed March 19, 2019.

13) Unger MA, Chou HP, Thorsen T, Scherer A, Quake SR. Monolithic microfabricated valves and pumps by multilayer soft lithography. *Science*. 2000;288(5463):113-116. http://www.ncbi.nlm.nih.gov/pubmed/10753110. Accessed March 18, 2019.

14) Peng C, Wang Y, Sungtaek Ju Y. Finger-powered electrophoretic transport of discrete droplets for portable digital microfluidics. *Lab Chip*. 2016;16(13):2521-2531. doi:10.1039/C6LC00219F

15) Xiang Z, Wang H, Pastorin G, Lee C. Development of a Flexible and Disposable Microneedle-Fluidic-System With Finger-Driven Drug Loading and Delivery Functions for Inflammation Treatment. *J Microelectromechanical Syst*. 2015;24(3):565-574. doi:10.1109/JMEMS.2015.2429675

16) Dal Dosso F, Kokalj T, Belotserkovsky J, Spasic D, Lammertyn J. Self-powered infusion microfluidic pump for ex vivo drug delivery. *Biomed Microdevices*. 2018;20(2):44. doi:10.1007/s10544-018-0289-1

17) Xu K, Begley MR, Landers JP. Simultaneous metering and dispensing of multiple reagents on a passively controlled microdevice solely by finger pressing. *Lab Chip*. 2015;15(3):867-876. doi:10.1039/C4LC01319K

18) Li W, Chen T, Chen Z, et al. Squeeze-chip: a finger-controlled microfluidic flow network device and its application to biochemical assays. *Lab Chip*. 2012;12(9):1587. doi:10.1039/c2lc40125h

19) Whulanza Y, Aditya R, Arvialido R, Utomo MS, Bachtiar BM. Ease fabrication of PCR modular chip for portable DNA detection kit. In: *AIP Conference Proceedings*. Vol 1817. AIP Publishing LLC ; 2017:040006. doi:10.1063/1.4976791

20) Whulanza Y, Nadhif H, Istiyanto J, Supriadi S, Bachtiar B. PDMS Surface Modification Using Biomachining Method for Biomedical Application. *J Biomimetics, Biomater Biomed Eng*. 2016;26:66-72. doi:10.4028/www.scientific.net/JBBBE.26.66

21) Nadhif MH, Whulanza Y, Istiyanto J, Bachtiar BM. Delivery of Amphotericin B to <i>Candida albicans</i> by Using Biomachined Lab-on-a-Chip. *J Biomimetics, Biomater Biomed Eng*. 2017;30:24-30. doi:10.4028/www.scientific.net/JBBBE.30.24

22) Whulanza Y, Kiswanto G, Safirna Widyaratih D, Istiyanto J, Kiswanto G. Realization and Testing of Lab-on-Chip for Human Lung Replication. *ARPN J Eng Appl Sci*. 2014;9(11). www.arpnjournals.com. Accessed March 19, 2019.

23) Whulanza Y, Aditya R, Arvialido R, Utomo MS, Bachtiar BM. Ease fabrication of PCR modular chip for portable DNA detection kit. In: *AIP Conference Proceedings*. Vol 1817. AIP Publishing LLC ; 2017:040006. doi:10.1063/1.4976791

24) Laser DJ, Santiago JG. A review of micropumps. *J Micromechanics Microengineering*. 2004;14(6):R35-R64. doi:10.1088/0960-1317/14/6/R01

25) Sollier E, Murray C, Maoddi P, Di Carlo D. Rapid prototyping polymers for microfluidic devices and high pressure injections. *Lab Chip*. 2011;11(22):3752. doi:10.1039/c1lc20514e